Journal of Statistical Physics, Vol. 65, No. 5/6, 1991

Population Growth in Random Media. II. Wavefront Propagation

A. Greven[1] **and F. den Hollander**[2]

In this second part of a two-part presentation, we continue with the model introduced in Part I. In this part, the initial configuration has one particle at each site to the left of 0 and no particle elsewhere. The expected number of particles observed at a site moving at speed $\tau \geqslant 0$ has an exponential growth rate (speed-τ growth rate) that is computed explicitly. The result reveals two characteristic wavefront speeds: τ_1, the speed of the front of zero growth (rightmost particle), and τ_2, the speed of the front of maximal growth. The latter speed exhibits a phase transition, changing from zero to positive as the drift in the migration crosses a threshold. The qualitative shape of the growth rate as a function of τ changes as well. In particular, below the threshold there appears a linear piece, which corresponds to the system exhibiting an intermittency effect.

KEY WORDS: Wave front propagation; random medium; variational formula; population growth.

3. INTRODUCTION AND RESULTS

3.1. Wavefronts

Our aim in Part II is to describe how the population in the model introduced in Part I spreads out in space in the course of time. For that purpose we choose the simple starting configuration

$$\eta_0(x) = \begin{cases} 1 & \text{for} \quad x \leqslant 0 \\ 0 & \text{for} \quad x > 0 \end{cases}$$

[1] Institut für Mathematische Stochastik, Universität Göttingen, W-3400 Göttingen, Germany.
[2] Mathematisch Instituut, Rijksuniversiteit Utrecht, 3508 TA Utrecht, The Netherlands.

0022-4715/91/1200-1147$06.50/0 © 1991 Plenum Publishing Corporation

and we investigate how this wavefront propagates to the right. There are *two characteristic wavefront speeds* of interest:

1. τ_1, the speed of the front of zero growth (rightmost particle).
2. τ_2, the speed of the front of maximal growth.

We shall refer to these as the *microscopic*, resp. *macroscopic*, wavefront speeds. It will turn out that whenever $\lambda(\beta; h; 0) > 0$ [see (0.20) of Part I]

$$0 \leqslant \tau_2 < \tau_1 \leqslant 1$$
$$\tau_2 \begin{cases} = 0 & \text{for} \quad h \leqslant h_c \\ > 0 & \text{for} \quad h > h_c \end{cases} \tag{3.1}$$

with h_c defined in (0.16) of Part I. In addition, the speed-τ growth rate (particle density profile) will be found to exhibit a nonanalyticity in the form of a *linear piece* when $h < h_c$ and $\theta_c > 0$, with θ_c defined in (0.17).

For earlier work on wavefronts in models of branching diffusion in an inhomogeneous medium we refer to Lalley and Sellke[1,2] and Dawson *et al.*[3]

3.2. Speed-Dependent Growth Rate

In (0.5) we defined $\lambda^{\text{II}}(\tau, F)$ as the exponential growth rate of the expected number of particles at site $\lfloor \tau n \rfloor$ (recall the remark below Theorem 1). In Theorem 1, (0.12), we found that

$$\lambda^{\text{II}}(\tau, F) = \lambda(\beta, h; \tau) \qquad F\text{-a.s.} \tag{3.2}$$

with the rhs given by the variational formulas (0.13) and (0.14). Our solution of (0.14) obtained in Proposition 4, (2.2), and Proposition 5, (2.17)–(2.18), now allows us to compute $\lambda(\beta, h; \tau)$. We use the notation in (0.15)–(0.16) and introduce an extra quantity $s^* = s^*(\beta, \tau)$ defined as follows:

$$\begin{aligned} \tau \leqslant \theta_c&: \qquad s^* = 0 \\ \tau > \theta_c&: \qquad s^* \text{ is the unique solution of } \tau = -\frac{F(s^*)}{F'(s^*)} \end{aligned} \tag{3.3}$$

Theorem 2 II. (i) The speed-τ growth rate is

$$\begin{aligned} \lambda(\beta, h; \tau) &= \lambda(\beta, h; 0) = \log[M(1-h)] + r^* && \text{if} \quad h > h_c, \tau \leqslant \theta^* \\ &= \log[M(1-h)] + s^* - \tau \log\left(\frac{1-h}{hF(s^*)}\right) && \text{otherwise} \end{aligned} \tag{3.4}$$

(ii) The maximizers $\bar{\theta} = \bar{\theta}(\beta, h, \tau)$ and $\bar{v}(\beta, h, \tau)$ are

$$\bar{\theta} \begin{cases} = \theta^* & \text{if} \quad \tau \leqslant \theta^* \\ = \tau & \text{if} \quad \tau > \theta^* \end{cases} \tag{3.5}$$

$$\bar{v}(i, j) \begin{cases} = \pi_{\xi^*}(i)\, \beta(j) & \text{if} \quad h > h_c, \quad \tau \leqslant \theta^* \\ = \pi_{\zeta^*}(i)\, \beta(j) & \text{otherwise} \end{cases} \tag{3.6}$$

with

$$\xi^* = 1 - \frac{j}{M} e^{-r^*} \qquad \text{and} \qquad \zeta^* = 1 - \frac{j}{M} e^{-s^*}$$

Corollary 2 II. (iii) $\tau \to \lambda(\beta, h; \tau)$ is continuous on $[0, 1]$, constant on $[0, \theta^*]$, strictly decreasing and analytic on $(\theta^*, 1)$, and at the endpoint $\lambda(\beta, h; 1) = \log h + \sum_j \beta(j) \log j$.

(iv) At $\tau = \theta^*$

$$\begin{aligned} \frac{\partial}{\partial \tau} \lambda(\beta, h; \theta^* +) &= 0 & \text{if} \quad h > h_c \\ &= -\log\left(\frac{(1-h)\, h_c}{h(1-h_c)}\right) & \text{if} \quad h \leqslant h_c \end{aligned} \tag{3.7}$$

(v) If $\lambda(\beta, h; 0) > 0 > \log h + \sum_j \beta(j) \log j$, then $\lambda(\beta, h; \tau)$ as function of τ changes sign at τ_c^*, the unique solution of $\lambda(\beta, h; \tau) = 0$ computable from (3.4).

Thus we see that the growth rate and the maximizers display interesting behavior as a function of τ for fixed β and h. This is displayed in the qualitative pictures in Figs. 1 and 2. Note that $\lambda(\beta, h; \tau) = \lambda(\beta, h; 0)$ for $\tau < 0$ trivially because $\eta_0(x) = 1$ for $x \leqslant 0$ and particles cannot move to

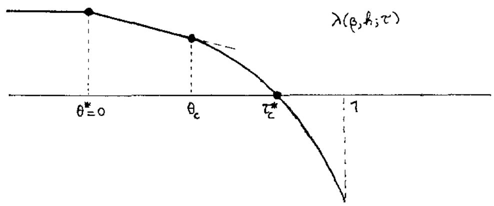

Fig. 1. The speed-τ growth rate $\lambda(\beta, h; \tau)$ as a function of τ for fixed β and h under the assumption (3.8) below, for $h < h_c$.

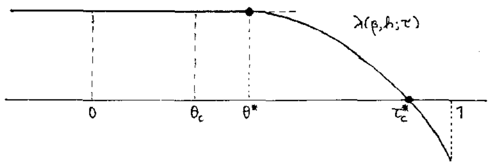

Fig. 2. As in Fig. 1, for $h > h_c$.

the left. The figures are drawn for the most interesting case where β and h are chosen such that

$$\begin{gathered}\sum_j \beta(j)\left(1-\frac{j}{M}\right)^{-1} < \infty \\ \lambda(\beta, h; 0) > 0 > \log h + \sum_j \beta(j) \log j\end{gathered} \tag{3.8}$$

implying that $0 < \theta_c < h_c < 1$ and $0 < \tau_c^* < 1$.

3.3. Interpretation of Phase Diagram

Two particularly interesting features of the above figures are: (1) As h crosses the critical value h_c the horizontal part of the curve reaches beyond 0; (2) for $h < h_c$ the curve has a linear piece in the interval $(0, \theta_c)$. In order to discuss these effects, we introduce the following notions.

Define

$$\tau_1 = \sup\{\tau: \lambda(\beta, h; \tau) > 0\} \tag{3.9}$$

$$\tau_2 = \sup\{\tau: \lambda(\beta, h; \tau) = \lambda(\beta, h; 0)\} \tag{3.10}$$

These are the microscopic, resp. macroscopic, wavefront speeds mentioned in Section 3.1. From Theorem 2II and Corollary 2II we obtain the following identification:

$$\begin{gathered}\tau_1 = \tau_c^* \\ \tau_2 = \theta^*\end{gathered} \tag{3.11}$$

In analogy with Section 0.5, we can define the *speed-τ typical path of descent* as the path of descent of a particle drawn randomly from the population at site $\lfloor \tau n \rfloor$ at time n (conditioned on it not being empty). Similarly, introduce its backward displacements relative to site $\lfloor \tau n \rfloor$

$$\hat{Z}^{n,\tau} = (\hat{Z}_i^{n,\tau})_{i=0}^n \qquad (\hat{Z}_0^{n,\tau} = 0) \tag{3.12}$$

and the two functionals

$$\hat{\theta}_n^\tau = \frac{1}{n} \hat{Z}_n^{n,\tau} \tag{3.13}$$

$$\hat{v}_n^\tau = \frac{1}{\hat{Z}_n^{n,\tau}+1} \sum_{x=0}^{\hat{Z}_n^{n,\tau}} \delta_{(\hat{l}_n^\tau(x),\, b_{\lfloor \tau n \rfloor - x})} \tag{3.14}$$

with $\hat{l}_n^\tau(x)$ its local time at site x [recall (0.26)–(0.28)]. The analysis in Section 1 shows that as $n \to \infty$, in analogy with (0.30),

$$\begin{aligned} &\hat{\theta}_n^\tau \to \bar{\theta}(\tau) \qquad \text{a.s.} \\ &\hat{v}_n^\tau \to \bar{v}(\tau) \qquad \text{in law for } \tau > 0 \end{aligned} \tag{3.15}$$

where $\bar{\theta}(\tau)$ and $\bar{v}(\tau)$ are the maximizers in (3.5) and (3.6) (for a rigorous treatment the tools can be found in Baillon *et al.*,[4] Section 3).

We now come to the discussion of the phase diagram.

(*I*) *Microscopic Wavefront.* The speed τ_1 tells us how fast the borderline of the population moves to the right.

Let

$$R_n = \sup\{x\colon \eta_n(x) > 0\} \tag{3.16}$$

be the position of the rightmost particle at time n. For any τ, every $\varepsilon > 0$, and n sufficiently large,

$$\begin{aligned} P(R_n > \lfloor \tau n \rfloor \mid F) &= P\Big(\sum_{x > \lfloor \tau n \rfloor} \eta_n(x) \geqslant 1 \mid F \Big) \\ &\leqslant \sum_{x > \lfloor \tau n \rfloor} E(\eta_n(x) \mid F) \\ &\leqslant (n - \lfloor \tau n \rfloor) \exp(n[\lambda(\beta, h; \tau) + \varepsilon]) \qquad F\text{-a.s.} \end{aligned} \tag{3.17}$$

The last inequality uses $\eta_n(x) = 0$ for $x > n$ plus the following observation. Let $x(n) \in (\tau n, n]$ be the site where $E(\eta_n(x) \mid F)$ is maximal. Let y be any weak limit point of $x(n)/n$ as $n \to \infty$. Then by the remark made below Theorem 1 the growth rate at $x(n)$ equals $\lambda(\beta, h; y)$. Since $y \geqslant \tau$, Corollary 2II(iii) gives $\lambda(\beta, h; y) \leqslant \lambda(\beta, h; \tau)$, which proves the claim. It follows from (3.17) and Corollary 2II(v) that

$$\limsup_{n \to \infty} \frac{R_n}{n} \leqslant \tau_c^* = \tau_1 \qquad \text{a.s.} \tag{3.18}$$

To prove the opposite inequality, we would have to show that $\lambda(\beta, h; \tau) > 0$ implies $\eta_n(\lfloor \tau n \rfloor) \to \infty$ a.s. (compare with the remark below Fig. 2 in Section 0.5 of Part I). Indeed, then

$$\{R_n \geqslant \lfloor \tau n \rfloor\} \supseteq \{\eta_n(\lfloor \tau n \rfloor) \geqslant 1\} \tag{3.19}$$

together with Corollary 2II(v) would imply

$$\liminf_{n \to \infty} \frac{R_n}{n} \geqslant \tau_c^* = \tau_1 \qquad \text{a.s.} \tag{3.20}$$

so that τ_1 could be identified with the speed of R_n. We defer this point to a future paper.

(II) *Localization vs. Delocalization of Macroscopic Wavefront.* By (3.11), $\tau_2 = \theta^*$. Since, by (0.19), $\theta^* = 0$ for $h \leqslant h_c$ and $\theta^* > 0$ for $h > h_c$, we see that the macroscopic wavefront develops a positive speed as h crosses h_c.

(III) *Intermittency.* The linear piece in Fig. 1 is related to a remarkable phenomenon for the speed-τ typical path of descent $\hat{Z}^{n,\tau}$. Indeed, it turns out that for $h < h_c$ and $\tau \in (0, \theta_c)$ there exist random subsets $A_n \subset [0, \hat{Z}_n^{n,\tau}]$ such that

$$\begin{aligned} &\lim_{n \to \infty} \frac{|A_n|}{|[0, \hat{Z}_n^{n,\tau}]|} = 0 \qquad \text{a.s.} \\ &\limsup_{n \to \infty} \frac{1}{n} \sum_{x \notin A_n} \hat{l}_n(x) \leqslant \frac{\tau}{\theta_c} \qquad \text{a.s.} \end{aligned} \tag{3.21}$$

(again we refer to Baillon *et al.*,[4] Section 3). Recall that $n^{-1}\hat{Z}_n^{n,\tau} \to \bar{\theta} = \tau$ by (3.5) and (3.15), because $\theta^* = 0$ when $h < h_c$. Equation (3.21) says that the path spends a positive fraction of its time on a subset of its range that has a density tending to zero. Thus, its *local times develop large peaks on a thin set*. This phenomenon is an example of intermittency.[5] The reason behind (3.21) is (3.6). Namely, if $\tau \in (0, \theta_c)$, then $s^* = 0$ by (3.3). Therefore $\bar{v} \in M_{\theta_c, \beta}$ [recall $\theta_c^{-1} = \sum_j \beta(j)(1 - j/M)^{-1}$], so that in particular $\bar{v} \notin M_{\bar{\theta}, \beta}$ because $\bar{\theta} = \tau$. This means that the supremum over v in Theorem 1, (0.14), is not achieved, which explains the above degenerate limiting behavior.

4. PROOF OF THEOREM 2II AND COROLLARY 2II

Most of the work has been done in Part I.

Proof of Theorem 2II. According to Proposition 4, (2.1),

$$\lambda(\beta, h; \tau) = \sup_{[\tau, 1]} J_{\beta,h}(\theta) \qquad (\tau > 0) \tag{4.1}$$

The properties of $J_{\beta,h}(\theta)$ are listed in Proposition 6.

I. If $h < h_c$, then $\bar{\theta} = \tau$, which fits with (3.5) because $\theta^* = 0$. We must now distinguish between $\tau \leqslant \theta_c$ and $\tau > \theta_c$. From (2.15) and Proposition 5

$$\bar{v}(i, j) = \pi_{\zeta^*}(i)\, \beta(j) \tag{4.2}$$

with

$$\begin{aligned} \tau \leqslant \theta_c: &\qquad \zeta^* = 1 - \frac{j}{M} \\ \tau > \theta_c: &\qquad \zeta^* = 1 - \frac{j}{M} e^{-r} \quad \text{with } r \text{ the solution of } \tau = -\frac{F(r)}{F'(r)} \end{aligned} \tag{4.3}$$

These two cases appear as one in (3.6) by the definition of s^* in (3.3). From Proposition 4, (2.2),

$$\begin{aligned} \lambda(\beta, h; \tau) &= J_{\beta,h}(\tau) \\ &= \log[M(1-h)] - \tau \log\left(\frac{1-h}{h}\right) - \tau K(\tau) \end{aligned} \tag{4.4}$$

where by Proposition 5

$$\tau \leqslant \theta_c: \qquad K(\tau) = \log \frac{1}{F(0)} \tag{4.5}$$

$$\tau > \theta_c: \qquad K(\tau) = -\frac{r}{\tau} + \log \frac{1}{F(r)} \quad \text{with } r \text{ the solution of } \tau = -\frac{F(r)}{F'(r)}$$

Again these two cases appear as one in (3.4).

II. If $h = h_c$, then $\bar{\theta} = \tau$ for $\tau \geqslant \theta_c$, while $\bar{\theta} \in [\tau, \theta_c]$ for $\tau < \theta_c$. In the latter case τ is still a maximizer. Hence $\bar{v}$ and $\lambda(\beta, h; \tau)$ are the same as in case I.

III. If $h > h_c$, then (3.5) holds because $\theta^* > 0$ is the maximizer of $J_{\beta,h}(\theta)$. For $\tau \leqslant \theta^*$ the maximizer $\bar{\theta} = \theta^*$ coincides with Theorem 2I, (2.21), hence $\bar{\nu}$ with (0.22) and $\lambda(\beta, h; \tau) = \lambda(\beta, h; 0)$ with (0.20). For $\tau > \theta^*$ we again have $\bar{\theta} = \tau$ and the result is the same as in cases I and II. □

Proof of Corollary 2II. Statements (iii) and (v) are immediate from Proposition 6. Statement (iv) follows from (2.28), namely, for $\tau > \theta^*$,

$$\frac{\partial}{\partial\tau} \lambda(\beta, h; \tau) = \frac{\partial}{\partial\tau} J_{\beta,h}(\tau) = \log\left(\frac{hF(s^*)}{1-h}\right) \tag{4.6}$$

Let $\tau \downarrow \theta^*$. If $h \leqslant h_c$, then $\theta^* = 0$, hence $s^* \downarrow 0$ by (3.3). Substitute (0.16) to get (3.7). If $h > h_c$, then $\theta^* > \theta_c$, hence $s^* \downarrow r^*$ by (0.19) and (3.3). But $hF(r^*)/(1-h) = 1$ by (0.18). □

REFERENCES

1. S. Lalley and T. Sellke, Travelling waves in inhomogeneous branching Brownian motions. I, *Ann. Prob.* **16**:1051–1062 (1988).
2. S. Lalley and T. Sellke, Travelling waves in inhomogeneous branching Brownian motions. II, *Ann. Prob.* **17**:116–127 (1989).
3. D. A. Dawson, K. Fleischmann, and L. G. Gorostiza, Stable hydrodynamic limit fluctuations of a critical branching particle system in a random medium, *Ann. Prob.* **17**:1083–1117 (1989).
4. J.-B. Baillon, Ph. Clément, A. Greven, and F. den Hollander. A variational approach to branching random walk in random environment, *Ann. Prob.*, to appear.
5. J. Gärtner and S. A. Molchanov, Parabolic problems for the Anderson model. I. Intermittency and related topics, *Commun. Math. Phys.* **132**:613–655 (1990).